M.I. SAVCHUK*, O.V. FILATOV**, and O.A. SHMATKO

G.V. Kurdyumov Institute for Metal Physics of the N.A.S. of Ukraine,
36 Academician Vernadsky Blvd., UA-03142 Kyiv, Ukraine

* marina_savchuk@ukr.net, ** filatov@imp.kiev.ua

PHYSICAL REGULARITIES FOR CELLULAR PRECIPITATION OF Co-, Cu-, AND Pb-BASED SUPERSATURATED SOLID SOLUTIONS

The decomposition of supersaturated solid solutions through the cellular mechanism is considered in terms of physical regularities of this phenomenon. The general characteristics of this process are described. The mechanisms of nucleation and subsequent cell growth as well as kinetic parameters of processes are partially described. The influences of some external factors on cellular precipitation process and its stages are characterized. Particularly, the effects of annealing temperature and a third element on the cellular precipitation process are studied.

Keywords: supersaturated solid solutions, ageing, cellular decomposition, lamellar structure, kinetic parameters, staged precipitation.

1. Introduction

The rapid growth in some science and technology fields has resulted in strict requirements to the properties of next-generation structural materials. The contemporary materials science and physics of metals focus on developing materials with the best possible set of operational properties. Over many years, one of the main tasks has been to find optimal structures that leverage the most favourable combination of alloy properties when exposed to a particular factor or a combination of some external or internal factors (mechanical, physical, thermal, chemical, *etc.*)

The research of phase transformations in metals and alloys plays an important role in the development of materials with predetermined

properties. Therefore, an in-depth study of the processes affecting the formation of metallic materials structure, which determines their properties, is of both scientific and great practical importance. Among numerous problems that this area faces, the study of the alloys where precipitation in supersaturated solid solutions occurs by the cellular mechanism takes an important place.

Ageing, as a solid-state phase-transformation process, has long attracted the attention of scientists and practitioners. The technology of artificial ageing is one of the up-to-date and effective methods of heat treatment for metallic alloys, which increases the strength considerably.

Currently, we know some binary and multicomponent alloys where the ageing occurs by the cellular precipitation mechanism. They include such alloys as cobalt–aluminium, cobalt–tungsten, copper–titanium and many others that are widely used in modern industry and technology. Although decomposition by the cellular mechanism has been investigated for over 90 years, the study of cellular precipitation is still of both academic and practical interest. This is confirmed by a long list of research papers investigating this problem with the monograph [1] at the top, which describes both theoretical and experimental data on cellular precipitation mechanism known at the time this book was written and published in 1976.

Over recent years, the interest in cellular precipitation of supersaturated solid solutions has increased greatly, and the flow of information regarding research on this phenomenon in various aspects has grown accordingly.

The main objectives of this paper include presenting the updated information and clarified regularities that have become available during recent years in addition to the fundamental long-known data.

One of the main aims is to classify general influence patterns that various factors have on the initiation and further development of cellular precipitation of supersaturated solid solutions and, most notably to highlight the issue of temperature as a factor affecting the rate and stages of cellular precipitation, and also the doping that has an influence on this process.

2. General Characteristics and Concepts of Cellular Precipitation of Supersaturated Solid Solutions

The decomposition of supersaturated solid solutions is one of the physical phenomena used for the heat treatment of metallic alloys to improve a set of operational properties. In modern materials science and physics of metals, the alloy ageing mechanisms are divided mainly into continuous and discontinuous precipitation.

Table. **Commonly used terminology in several European languages**

Language	Study method	
	Microstructural analysis	X-ray analysis
Ukrainian	Комірковий розпад	Несталоплинний розпад
Russianя	Ячеистый распад	Прерывистый распад
English	Cellular precipitation	Discontinuous precipitation
German	Zellulär Entmischung	Diskontinuierlicher Ausscheidung
French	Décomposition cellulaire	Décomposition discontinue
Polish	Wydzielanie komurkowe	Przemiana niecięgła

This terminology is related to the pattern of changes that occurs in the initial solid solution concentration, which is usually registered by the x-ray method due to the change in a lattice parameter.

Continuous precipitation simultaneously occurs throughout the entire alloy bulk being controlled by the bulk diffusion of solute atoms, but the initial concentration of supersaturated solid solution decreases gradually during the isothermal annealing, approaching equilibrium at a given annealing temperature. The radiographic method registers the corresponding shift of the reflexes in the solid solution that occurs synchronously with the concentration change.

In the case of discontinuous precipitation in solid solutions, the x-ray diffraction pattern reveals a system of reflexes specific to depleted solid solutions. During the isothermal annealing, the intensity is pumped from the reflex system of the initial solid solution to the depleted system. Discontinuous precipitation is controlled by the grain boundary diffusion of solute atoms.

Cellular precipitation in supersaturated solid solutions is a common instance of discontinuous precipitation in solid solutions. This term is provided in several European languages in Table above.

2.1. Mechanism and Kinetics of Cellular Precipitation

Studying the ageing behaviour of silver–copper alloys in 1930s, N. Ageev, M. Hansen, and G. Sachs [2] first discovered a second pattern of x-ray reflexes matching the areas of depleted solid solutions in cells that some time during the ageing coexist with the reflex system of initial supersaturated solid solutions, while the intensity of reflexes gradually decreases in initial supersaturated solid solutions that increases in depleted solid solutions. The authors called this two-phase decomposition. Other researchers call this process as discontinuous precipitation (DP) due to the abrupt change in the crystal lattice. The more accurate microstructural studies gave grounds to call it cellular precipitation.

Fig. 1. The microstructure of Co−32 wt.% W alloy after 25.92·10⁴ s ageing at 875 K [11], where α_0 is an initial matrix of supersaturated solid solution with concentration c_0, α_c is the depleted solid solution with concentration c_c, and γ is a precipitation phase
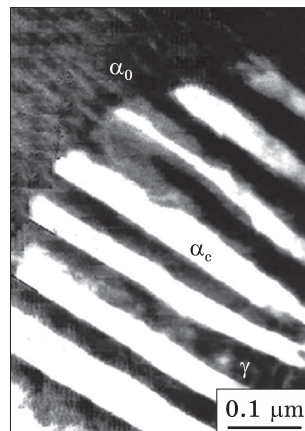
As in most cases, during a cellular precipitation process, metallography examination reveals reactions areas in the form of dark zones of increased etching. These areas occurring in polycrystalline materials, usually on the grain boundaries, A. Geisler [3] called nodules, and the very process of their formation and growth as a nodular reaction. Accepting G. Hardy's concept [4] that this process is induced by the matrix deformation, A. Geisler called this process a recrystallization reaction. This term might be quite acceptable if there had been no cases of cellular precipitation [1, 5] that occur without prior matrix hardening due to the general precipitation. The term 'grain boundary reaction' used in the Japanese literature [6] is even less accurate. D. Turnbull was the first to use the term cellular precipitation, replacing the word 'nodule' with 'cell'.

Cellular precipitation occurs on the high-angle grain boundaries because the structure of low-angle grain boundaries (with an angle below 15°) does not provide sufficient mobility to initiate cellular precipitation. This fact is confirmed in Refs. [8−10] using Pb−Sn alloys where the cells are not formed on the boundaries with misorientation less than 15°. In general, grain boundaries separate areas similar in phase and crystal structure, but different in orientation. Grain boundaries migration is quite similar to the growth of one crystal due to the absorption of a neighbouring one. In this sense, a grain boundary is a surface contact area of tangent grains.

Cellular precipitation is a process characterized by the formation and growth of eutectoid-like colonies, called cells (Fig. 1) that consist of depleted solid solution lamellae and a precipitation phase. Cellular precipitation occurs in a limited number of alloys (mostly in those that are double or triple) within a definite temperature range.

The microstructure of solid solution areas where decomposition occurs by the cellular precipitation mechanism is so similar to the microstructure of eutectoid reaction products that it is difficult to distinguish them by metallographic examination. This similarity explains some authors' tendency (see, *e.g.*, Ref. [12]) to consider cellular precipitation to be a case of a eutectoid reaction.
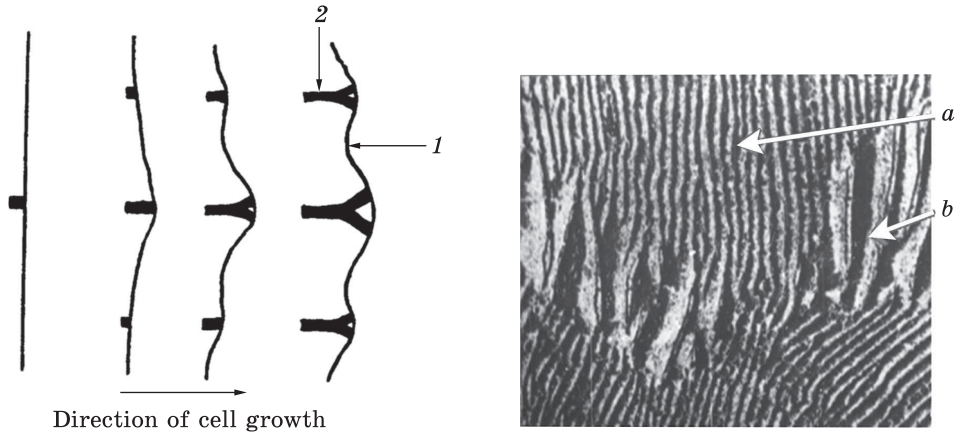
Fig. 2. Schematic of a cellular precipitate, where *1* is a cellular reaction front, and *2* are the branching lamellae occurred during the precipitation phase that derives a specific cell size [22]

Fig. 3. The structure of Al−49 wt.% Zn alloy with areas where the primary (*a*) and secondary (*b*) cellular reactions occurred [6]

However, it should be noted that there is a significant difference between the eutectoid reaction and cellular precipitation. During the eutectoid reaction, two new phases (β) and (γ) are formed from the matrix phase (α_0). During the cellular precipitation, the lamellae of only one new phase (γ) are formed, while another type of lamellae in the growing cell is represented by areas of phase (α_c). Therefore, the eutectoid reaction can be schematically represented as $\alpha_0 \rightarrow \beta + \gamma$, and the cellular precipitation as $\alpha_0 \rightarrow \gamma + \alpha_c$.

The cells formed following cellular precipitation include those that grow mainly on one side of a grain boundary during the ageing and those that grow on both sides of a grain boundary. Multiple microstructural studies indicate that cells in such alloys as aluminium−silver [13, 14], zinc−silver [6], zinc−copper [15, 16] develop on one side of a grain boundary, but in cobalt−tungsten [5, 17, 18], nickel−beryllium [19], lead−tin [5], lead−cadmium [20, 21] alloys develop on both sides of a grain boundary.

However, in both cases, the cells are basically identical, and, as a rule, these two types of cells coexist in alloys. In the alloys characterized by relatively rapid cellular precipitation, a greater number of cells grow on both sides of a grain boundary. The alloys characterized by a later occurrence of cellular precipitation, the most cells grow on one side of a grain boundary. This fact might be due to the crystallographic orientation of neighbouring grains.

The cell shape is quite complex. In the case when 'bilateral' cells are growing, a grain boundary, being compressed between the cells, takes a

tortuous *S*-shape. In the case when 'unilateral' cells are growing, the initial boundary mostly takes a serrated shape. Figure 2 gives a schematic of a cellular reaction front under migration during the ageing process.

Cellular precipitation colonies consist of precipitation phase lamellae (γ) and a depleted solid solution (α_c) with a concentration (c_c) that significantly exceeds the equilibrium concentration (c_i) as mentioned above. Thus, Pb−Sn alloys show that, during the initial cellular reaction, the solid solution decomposes only by 50−60% in concentration [7].

Residual supersaturation of the depleted solid solution initiates a secondary cellular reaction that results in cells characterized by a lower growth rate and less dispersed structure (Fig. 3). The figure shows that interlamellar spacing in secondary cells is three or even five times greater than the interlamellar spacing in primary cells. The secondary cellular reaction was observed in a number of alloys (Cu−Ti [23], Pb−Sn [24, 25], Al−49% Zn and Zn−38% Al [6], Cu−6.5% Ag [6], Fe−30% Ni−6% Ti [26−28], Cu−1.4% Be [29], Co−Ni [30]).

2.1.1. Cell Formation

As mentioned above, the cells are formed on high-angle grain boundaries in the alloys aged by cellular mechanism. P.J. Clemm and J.C. Fisher [31], within the framework of the classical theory of nucleation, computed the energy of this process for different parts of grain boundaries. It was shown that the nucleation energy is the smallest in the area near the grain vertex (four-grain junction) and increases with a successive transition to the dihedral angle at the edge between two surfaces (three-grain junction) and a simple grain boundary (two-grain junction). Thus, the grain vertices are the most favoured sides for nucleation.

It is clear that grain vertices and boundaries are quickly becoming depleted as nucleation sites. In addition, the nucleation rate depends on the atom density relative to a particular nucleation site, *i.e.*, atom density on the grain vertices is the lowest. Their density is consistently increasing on grain boundaries, boundary surface and inside the grain. Since the work done in formation of critical nucleus on the grain boundary surface is much lower than inside the grain, the nucleation occurs faster on the grain boundary, all other things being equal.

On grain boundaries, there are several areas characterized by different values of work done in the formation of a critical nucleus, as noted above. Since this nucleus growing process is easier and faster than its formation, provided that the nucleation sites are fairly large in number, the process started in sites having a minimum value of the Gibbs free energy of nucleus formation, will extend to all probable nuclei sites.

Given the relatively small proportion of probable predominant nucleation sites in relation to the total volume, it should be noted that a new phase nucleus formation rate should decrease over time as the nu-
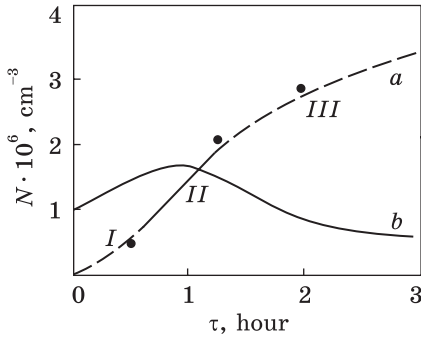
Fig. 4. Cell quantity *vs.* the time of isothermal annealing in Co−31.9 wt.% W alloy at 973 K, where the primary data (*a*) are given in Ref. [1]. *I* — nucleation process at a non-steady-state regime; *II* — nucleation process at a steady-state regime; *III* — attenuation of the nucleation process. The curve (*b*) is based on the first derivative of the origin function, which determines the nucleation rate

cleus sites are depleted or lose their effectiveness, if blocked by the growing transformation zone. This case has been investigated by M. Avrami [32].

Let us denote the number of probable predominant nucleation sites per matrix phase unit volume as $\breve{N}$; each of these sites let be characterized by some time-constant frequency of nucleation v_s. During the alloy ageing, nucleation sites of a new phase gradually deplete and, at the time (τ) of annealing, their number is as follows:

$$N_{\tau} = \breve{N}\left(1 - \exp(v_s \tau)\right). \tag{1}$$

Using differentiation (1), we obtain the nucleation rate of new phase centres:

$$\widehat{N} = \breve{N} v_s \exp(-v_s \tau). \tag{2}$$

Figure 4 shows the dependence of cell numbers on the time of isothermal annealing, where we can observe ranges (*I*, *II* and *III*) corresponding to three stages of a nucleation process. The first stage (*I*), the initial stage corresponds to the non-steady-state mode of this process. The second stage (*II*) corresponds to a linear section of the dependence, which describes the process in a steady-state mode with maximum velocity (curve (*b*) in Fig. 4). The beginning of the third stage (*III*) is associated with the attenuation of the nucleation process due to the gradual depletion of the predominant nucleation sites.

As shown on the examples of Co−31.89 wt.% W and Cu−4.35 wt.% Ti alloys [1, 5, 33, 34], the relationship between cell number and ageing time is sigma shaped.

As noted above, primary nucleus formation occurs at a non-steady-state mode. The time-dependence of unsteady nucleation rate was firstly studied by Ya.B. Zeldovich [35], who proposed the parameter of non-steady-state τ_H with a time dimension.

Taking into account a non-steady-state mode, we obtain:

$$N = \breve{N}\left(1 - \exp(-v_s e^{-\tau_H/\tau} \tau)\right). \tag{3}$$

Then, we have an equation for the nucleation rate:

$$\widehat{N} = v_s \breve{N} \exp\left(-\frac{\tau_H}{\tau} - v_s \tau e^{-\tau_H/\tau}\right)\left(1 + \frac{\tau_H}{\tau}\right), \qquad (4)$$

which was experimentally confirmed, *e.g.*, by studies in the formation of recrystallization centres of weakly deformed coarse-grained aluminium [36].

2.1.2. Cell Growth Process

Solute atoms get to the particular lamellar site through the boundary that goes around the upper side of these lamellae, stimulating its growth. With that, the boundary migrates synchronously with the growing lamellae. Microstructural studies show that lamellae in the cells of many alloys are not completely straight and parallel, but seem to be branching, deriving the increasing diameter of the cell.

However, the interlamellar spacing remains approximately constant due to the newly born lamellae. Different theories of cellular precipitation [7, 37–40] assume that a growing cell has a specific interlamellar spacing value that can provide the highest growth rate. In this regard, it is assumed [8] that when the local inter-lamellae spacing becomes quite large during the cell growth, another one forms on the moving boundary, which, according to [8], is ideal for a nucleation.

Figure 5 demonstrates the schematic of this process. This is a place where a new lamellar structure is formed to keep the interlamellar spacing close to constant. This constancy persists at a certain annealing temperature and alloy composition. However, if these parameters are changing, the spacing between the lamellae is also changing.

The first attempt to describe mathematically the growth rate of eutectoid colonies (v) through the initial concentration (c_0), equilibrium concentration (c_l), interlamellar spacing (l) and bulk diffusion coefficient (D_v) was Zener's equation [39]:

$$v = \frac{2(c_0 - c_l)D_v}{c_0 l}. \qquad (5)$$

According to the assumption that, during the cellular precipitation in supersaturated solid solutions, cell growth is controlled by grain boundary diffusion, Turnbull proposed a mathematical model for this growth [7]:
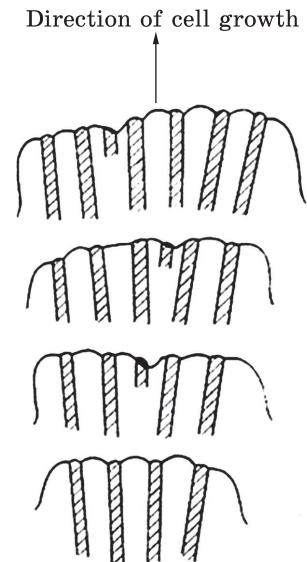

Direction of cell growth

Fig. 5. Scheme of keeping constant inter-lamellae spacing in the cell [1]

$$v = \frac{2(c_0 - c_c)\lambda D_b}{c_0 l^2}, \quad (6)$$

where D_b is a grain-boundary diffusion coefficient, λ is a grain boundary width (0.5 nm).

The experimental study satisfactorily confirmed Eq. (6) for cobalt–tungsten, nickel–beryllium [1], silver–copper [41], zinc–copper, and aluminium–silver (high silver) alloys [6]. With that, it was shown that D_b value is not a coefficient of grain boundary self-diffusion, but a coefficient of heterodiffusion across the migrating boundary interface. The research papers [42, 43] confirm the above conclusion showing that atom diffusion mobility across the given surface can differ considerably from their mobility on the steady-state boundary. The change in the initial matrix concentration due to the total decomposition in some alloys significantly complicates the mechanism of cellular precipitation, and Eq. (6) cannot be used to describe cell growth kinetics. In this regard, we propose several variants of Eq. (6), taking into account the following parameters:

$$v = \frac{2(c_0 - c)\lambda D_b}{(c_0 - c_l)l^2} \ [40], \quad (7)$$

$$v = \frac{2(c_i - c_l)\lambda D_b}{(c_i - c_0)l^2} \ [44], \quad (8)$$

$$v = \frac{4\lambda D_b}{l^2} \ [44], \quad (9)$$

$$v = \frac{-8\Delta Gs\lambda D_b}{RTl^2} \ [45], \quad (10)$$

$$v \propto \frac{\lambda D_b}{l^3} \ [46], \quad (11)$$

$$v \propto \frac{\lambda D_b}{l^4} \ [47]; \quad (12)$$

here, c_i — content of impurities in the precipitation phase, s — segregation factor, R — gas constant, T — absolute temperature, ΔG —sum of changes in chemical free energy ΔG_x and surface free energy on the interphase surface ΔG_σ, *i.e.*,

$$\Delta G = \Delta G_x + \Delta G_\sigma. \quad (13)$$

The set of formulas related to the parameter of cell growth rate has shown the ability to use different approaches to its description, but

all of them use a heterodiffusion coefficient across the migrating grain boundary.

After analysing the equations that mathematically describe a growth rate of eutectoid colonies, it becomes clear that majority of them do not explicitly include temperature as a parameter. It is common knowledge that temperature being an external factor has a significant impact on diffusion processes and, accordingly, on their parameters. In particular, in this case, the temperature factor is closely related to the coefficient of heterodiffusion across the migrating grain boundary, which is a component of the above equations. It should be noted that cellular ageing refers to the diffusion processes. The cellular precipitation of supersaturated solid solutions is typically associated with the diffusion of solute atoms along the grain boundaries. Thus, the temperature indirectly causes a significant impact on the cellular precipitation process.

Regarding the concept that bulk diffusion (D_v) is a factor controlling a cellular precipitation rate in supersaturated solid solutions, the following should be noted. In Ref. [48], where the Co−W system was investigated in the temperature range from 870 to 1070 K, in which the ageing occurs by the cellular mechanism, the bulk diffusion coefficient (D_v) was determined. The calculated values were three orders of magnitude greater than the experimental values for the same parameter.

A lack of correlation between results makes us conclude that attempts to describe the kinetics of cellular precipitation *via* bulk diffusion are groundless.

As observed, the bulk diffusion has some impact on the cellular precipitation as the ageing temperature is rising. However, at high temperatures, it eventually stops the cellular precipitation in solid solutions and causes the transition to the intensified decomposition in the alloy bulk.

2.1.3. General Kinetics of Cellular Precipitation in Supersaturated Solid Solutions

The general kinetics of cellular precipitation in supersaturated solid solutions is described mainly by two parameters: cell nucleation rate $\widehat{N}$ and cell growth rate v, *i.e.*, front migration rate of the cellular reaction.

In addition, the general kinetics of cellular precipitation, as shown in Ref. [1], reasonably fits J. Cahn's theory and is described by the equation:

$$V_{tr} = 1 - \exp V_s, \qquad (14)$$

where V_{tr} is a volume of the transformed alloy, V_s is the sum of all cell volumes, related to the total alloy volume and associated with $\widehat{N}$ and v as follows:
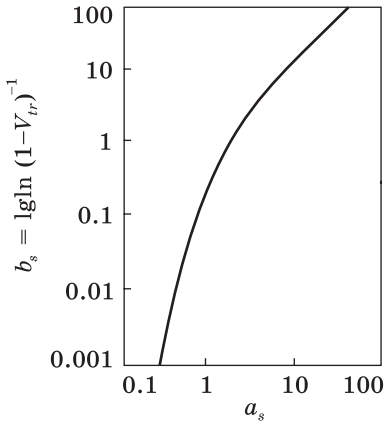
$$V_s = b_s^{1/3} f_s(a_s), \qquad (15)$$

Fig. 6. J. Cahn's characteristic curve [49]

where

$$a_s = (I_s v^2)^{1/3} \tau,$$

$$b_s = \frac{I_s}{8S^3 v} = \frac{\widehat{N}}{8S^4 \tau};$$

$$(16)$$

I_s is the stationary nucleation rate of new phase per grain boundary unit area, S is a grain surface area per unit volume that constitutes $3.35D^{-1}$ (D is an average grain diameter).

Plotting Eq. (14) on a logarithmic scale gives a curve with an inflection (Fig. 6).

Cellular precipitation of supersaturated solid solutions belongs to that type of processes, during which the predominant nucleation sites are getting depletion in the initial stages. The lower part of the Cahn's curve (Fig. 6) corresponds to the nucleation stage and cell growth, the curve inflection is related to the depletion of nucleation sites, whereas further process occurs only due to the growth of formed nuclei (upper part of Cahn's curve).

3. Methods for Studying the Cellular Precipitation Mechanism

The quantitative statistical metallography, x-ray diffraction analysis, dilatometry, resistometry, and others are methods commonly used in the isothermal regime to obtain general kinetics data on the processes related to the cellular precipitation in supersaturated solid solutions.

The cell growth is studied by the method of quantitative statistical metallography. The measurement data are used to build the isothermal dependencies of the maximum cell size in the direction of their growth (L_{max}) on the annealing time (τ). This type of function is usually linear (Fig. 7).

The function $L_{max} = L_{max}(\tau)$ often cuts off a certain segment τ_0 on the time axis. The value of τ_0 is a latent period (the time when the process is developing to the stages when its observation becomes possible). Therefore, in general, the value of v [m/s] is described by the equation

$$v = \frac{L_{max}}{\tau - \tau_0}.$$

$$(17)$$

The interlamellar spacing is determined by the method [50]. Since the metallographic section does not generally intersect the package of lamellae that forms the cell at right angle, the value of the observed interlamellar spacing l_a is always greater than its true value. Therefore,
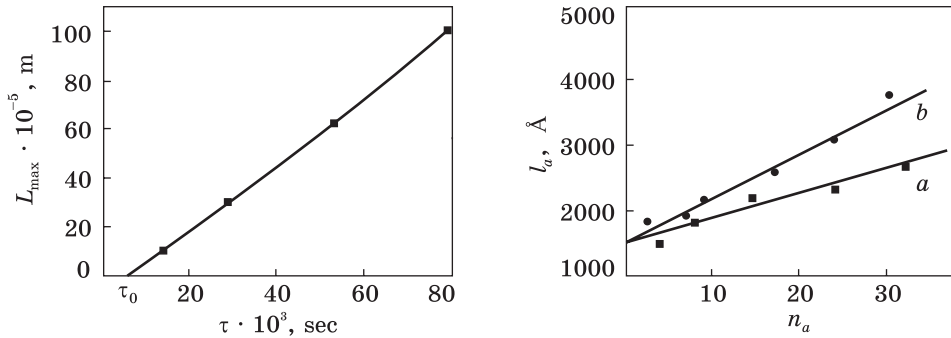
Fig. 7. The time-dependence of L_{max} for Co−31.89 wt.% W alloy at 873 K [5]

Fig. 8. The $l_a = l_a(n_a)$ dependencies for Co−14.65 wt.% W annealed for 6 (*a*) and 12 (*b*) hours at 973 K [1]

a real l is determined based on a set of measurements (approximately in 30−50 cells) of the l_a value and the dependency graph $l_a = l_a(n_a)$ (Fig. 8) where n_a is the number of inter-lamellar spacing values that are less than a given value of l_a. Generally, the $l_a = l_a(n_a)$ function is linear, and the value of l is determined by the point of its intersection with the *y*-axis.

Figure 8 shows dependence for determining the true inter-lamellar spacing using the above method. The lines mean the annealing time of 6 hours (*a*) and 12 hours (*b*) at 973 K. Since the value of a true interlamellar spacing is determined by the intersection point of $l_a = l_a(n_a)$ curve with the *y*-axis, l is of 1500 Å.

4. Temperature Effect on the Process of Cellular Precipitation Initiation and Growth

Generally, cellular precipitation is associated with the initial supersaturated solid solution and grain boundaries migration, which is determined by their structure.

Along with that, a temperature is an important factor. Using the example of any given system, cellular precipitation in a supersaturated solid solution occurs in a certain temperature range that is characteristic to the studied alloy [1].

Figure 9 illustrates temperature ranges for the ageing process that occurs by the cellular mechanism for Co−W, Co−Al, and Cu−Ti alloys relative to the melting temperature of the respective alloys.

However, we should remember that increase in the annealing temperature, in addition to accelerating cellular precipitation process, leads to initiating other ageing mechanisms.

As clearly shown in Fig. 9, the phenomenon of cellular precipitation occurs in the average temperature range, which is characterized by a
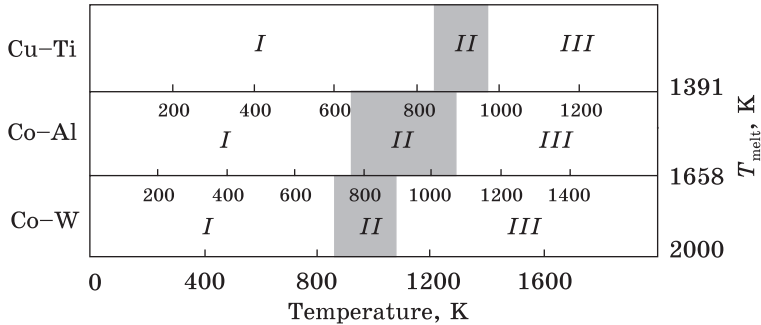
Fig. 9. Temperature ranges for the ageing process that occurs by the cellular mechanism for Co–W, Co–Al, and Cu–Ti alloys. Here, *I* — slow diffusion processes area, cellular precipitation is not occurring; *II* — the area of ageing process by the cellular mechanism; *III* — decomposition in the bulk

slower diffusion rate in the grain bulk than on the grain boundaries. As the temperature rises, the atom diffusion mobility in the grain bulk increases. This contributes to the intensification of the overall decomposition of the solid solution, competing with the cellular mechanism. As a result, the degree of supersaturation in solid solutions reduces in front of the growing cells and the force that causes cellular precipitation decreases. The cellular precipitation rate decreases, and with the subsequent temperature rise, the cellular precipitation completely stops.

As shown in Ref. [51], as the annealing temperature increases, the cellular precipitation rate decreases due to the intensification of decomposition in the alloy bulk that, at a certain temperature, completely inhibits cellular precipitation.

Generally, the cellular precipitation in a supersaturated solid solution that occurs in any given system is associated with a certain temperature range in which this process is possible (Fig. 9). Reducing the temperature below this range is associated with diffusion slowdown, however, its increase is connected with the cellular precipitation suppression by other its types.

4.1. Effect of Cooling Rate on the Cellular Precipitation Process

In general, a cooling rate during the heat treatment can affect both the phase transformations and the mechanical properties of the alloys [52]. Nevertheless, in most cases, the experimental research is conducted to investigate the effect of quenching media temperature, which affects the cooling rate, taking into account the thermal properties of the material. The quenching media temperature also affects the cellular precipitation process, in particular, its rate. In Ref. [53], on an example of Co–31.89 wt.% W system, authors showed that the cell growth rate increases with an increasing cooling rate of the alloy. For the samples that were annealed immediately after cooling from the homogenization area

to the ageing temperature, the cell growth rate is of $2.3 \cdot 10^{-7}$ cm/s, but for water-quenched samples it exceeds $9.4 \cdot 10^{-7}$ cm/s, however, quenching in liquid nitrogen increases the cell growth rate to $2.8 \cdot 10^{-6}$ cm/s. Besides, liquid nitrogen quenching significantly accelerates the cell formation process. It can be seen that an increase in the cooling rate relative to the quenching media temperature results in significant acceleration of the cell growth.

Residual stresses occur within metals as a result of rapid hardening. Under the emerging stresses, migration of existing dislocations is activated and new dislocations are generated [54]. These processes can accelerate both self-diffusion [55, 56] and heterogeneous diffusion of interstitial atoms [57, 58] and substitutional atoms [59]. In addition, due to this type of heat treatment, the concentration of point defects that significantly exceeds the equilibrium is retained. It also accelerates diffusion processes, and therefore the process of cellular precipitation, which is associated with changes in bulk.

4.2. Effect of Temperature on the Cellular Precipitation Stages

In contrast to steady-state decomposition, cellular precipitation occurs in stages. The question of stages is considered fundamentally in the study of cellular precipitation in supersaturated solid solutions [60, 61].

The structure of primary and secondary cellular reactions differs significantly in dispersibility, as mentioned at the beginning of this paper. This aspect has received little attention before. Actually, this is what caused a certain dilemma. This dilemma is related to the incorrect approach to the study of ageing behaviour of supersaturated solid solutions by the cellular mechanism. Specifically, it consists in a significant difference between data obtained from the transformed area of a metallographic section and a transformed bulk. The point is that, in terms of metallography, the cellular precipitation process was considered complete after analysing only transformed area of a metallographic section, which was filled with overgrown cells formed as a result of ageing. However, at the same time, volumetric changes continued to occur, indicating that the process of cellular
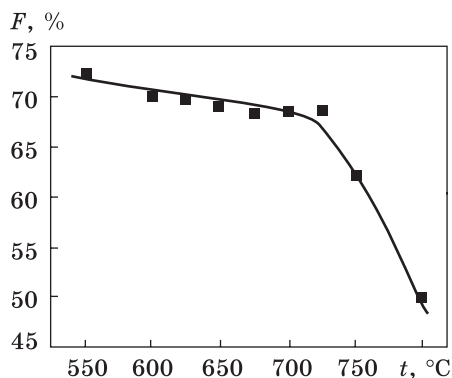
Fig. 10. Temperature-dependent decomposition degree in the supersaturated Co−12.71 at.% Al during the primary cellular reaction [64]
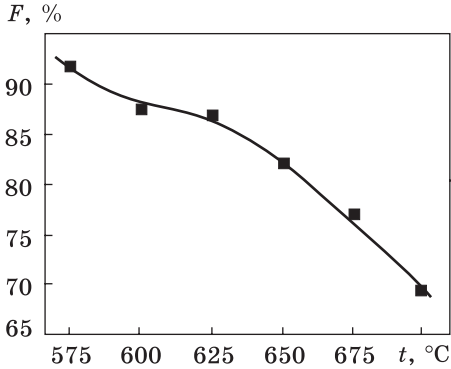
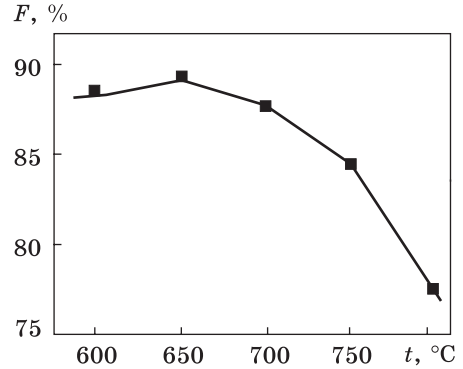**Fig. 11.** The same as in the previous figure, but for Cu−6 at.% Ti [65]

Fig. 12. The same as in the previous figure, but for Co−13 at.% W [66]

precipitation was still incomplete. We can use several techniques, such as resistometry, dilatometry, and x-ray diffraction analysis to investigate further this process. However, this dilemma can be resolved when we separate primary and secondary cellular reactions.

In Refs. [62, 63], on the example of Pb−Sn system, the primary and secondary cellular reactions are separated, their time intervals and kinetic parameters are determined.

The effect of temperature on the stages of a cellular precipitation process in supersaturated solid solutions is quite significant. In Ref. [64], the percentage of the decomposed supersaturated solid solution following the primary cellular reaction was determined in function to the ageing temperature of Co−12.71 at.% Al alloy. Figure 10 illustrates temperature-dependent decomposition in the supersaturated solid solution.

This dependence shows that a degree of decomposition gradually decreases with the increasing ageing temperature in the investigated alloy. The initiation and behaviour of the secondary cellular reaction is influenced by the volume of residual supersaturation in the solid solution caused by the degree of decomposition that occurs in the primary cellular reaction. That is why the probability of the secondary reaction increases with increasing the aging temperature.

A similar pattern was observed on the example of Cu−6.0 at.% Ti alloy [65] and Co−13.00 at.% W alloy [66]. The temperature-dependent decomposition degree in the supersaturated solid solution for Cu−6.0 at.% Ti alloy is given in Fig. 11.

The temperature-dependent decomposition degree in the supersaturated solid solution for Co−13.00 at.% W alloy is given in Fig. 12.

Therefore, the primary cellular reaction that occurs at high temperatures creates favourable conditions for the initiation of a secondary cellular reaction.

264

5. Effect of the Third Element
on the Cellular Decomposition Process

One of the fundamental issues in the research of phase and structural transformation kinetics, specifically, recrystallization, growth of grains, cellular precipitation in supersaturated solid solutions, is the analysis of a third element doping. Given that a third element doping allows controlling the decomposition process of supersaturated solid solutions [1], this issue is quite important in the study of ageing by the cellular mechanism.

In Ref. [67], the effect of a third element on the acceleration or deceleration of the cellular precipitation process was highlighted. During the study of kinetics of the cellular precipitation on the example of Co−9.65 at.% W alloy, the growth rates of alloy cells doped with different elements are obtained. The alloys doped with 1.21 at.% Ni, 1.12 at.% Cu, 1.48 at.% Ti, and 0.78 at.% Zr are studied. Taking into account that the cell growth rate of Co−9.65 at.% W alloy is of $5.6 \cdot 10^{-9}$ m/s, the data analysed in this paper demonstrate a mixed impact of the doping elements. Thus, it was found that doping with Ni and Cu (the cell growth rate of the alloy is $31.0 \cdot 10^{-9}$ m/s and $11.5 \cdot 10^{-9}$ m/s, respectively) accelerates the cellular precipitation of the alloy. Doping with Ti and Zr (the cell growth rate of the alloy is of $1.07 \cdot 10^{-9}$ m/s and $0.45 \cdot 10^{-9}$ m/s, respectively), on the contrary, slows down this process.

It should be noted that adding the doping element in different amounts within the same system has also a mixed impact on the cellular precipitation process. In Ref. [68], the effect of iron doping on the decomposition of a solid solution of Co−7 wt.% Al alloy was studied. The alloys doped with 1, 5, 10, and 20 wt.% Fe were studied. It was found that doping with 1 wt.% Fe significantly accelerates the cellular precipitation. For the 5 wt.% Fe doped alloy, in the initial stages, this process slows down. Thus, after this, alloy is annealed for, *e.g.*, one hour, and the cells occupy only 13% of metallographic section area, while in the binary alloy and in the alloy doped with 1 wt.% of Fe, this value is of 18% and 25%, respectively. In the alloy with 10 wt.% of Fe, the cellular precipitation occurs rather sluggishly. The alloy with 20 wt.% of Fe is characterized by the lack of any signs of cellular precipitation. It is obvious that doping with a small amount of iron accelerates the cellular precipitation process in the studied Co−7 wt.% Al alloy, but an increase in Fe to 10 wt.% significantly inhibits this process.

Regarding the acceleration or inhibition of the cellular reaction front migration by a third element, there are still no definitive and unambiguous evidence. Some advances made towards the explanation of acceleration or deceleration of cellular precipitation in a specific system, based on the analysis of atom-size difference, impurity maximum

solubility in the metal-matrix or its melting point cannot be confirmed generally for other systems.

Therefore, the research papers investigating the effect of a third element on the cellular precipitation, take a case-by-case approach when explaining this phenomenon in a specific case for a specific system. Particularity, the behaviour of impurity atoms is often attributed to the horophilicity or horophobicity.

After analysing the effect of doping on cellular precipitation in lead–tin (Pb–Sn) alloys, the authors [69] showed that horophobic (surface-inactive) impurities inhibit it, while horophilic (surface-active) impurities can both inhibit and accelerate this process. As mentioned above, this might be due to a number of reasons. The impact of atomic volumes, bond energy and the electronic structure in terms of energy benefits are among them.

The cellular reaction front rate should be a function of impurity atoms behaviour on or before that front, namely, their influence on the diffusion of other base element atoms. In Ref. [70], the behaviour of impurity atoms (associated with horophilicity or horophobicity) is characterized by statistically generalized atom moments [71], their difference between that for impurity element and that for matrix metal.

The attempts to describe the third element influence pattern associated with the concept of horophilicity or horophobicity include V.I. Arkharov hypothesis [72] that takes a worthy place. The phenomenon of defective areas enrichment (structural heterogeneity) of a solid with solute atoms, which leads to the decrease in excess energy of defects, is called as segregation without precipitation. According to V.I. Arkharov, this process is called an internal adsorption. This phenomenon is observed on the grain boundaries. The positive adsorption of dissolved impurities is called as horophilicity, and impurities that cause this activity are known as horophilic. In the case of horophobic impurities, the opposite behaviour is observed.

Since the findings regarding the effect of a third element on the cellular precipitation are ambiguous and mixed, it is difficult to give an obvious and clear explanation to this phenomenon. This problem remains an open and questionable to this day, although a long list of research papers are available. It might be due to the influence of other parameters not taken into account in the horophilicity concept.

6. Conclusions

The physical regularities of cellular precipitation of supersaturated solid solutions are generalized. The general characteristics of this phenomenon, nucleation mechanisms, subsequent growth of cells, and its kinetic parameters are described.

As demonstrated, an increase in the cooling rate relative to the quenching media temperature results in significant acceleration of cell growth. This aspect is due to the residual stresses in metals occurred following rapid hardening, which further accelerates the diffusion processes and, hence, the process of decomposition by the cellular mechanism.

The varied findings regarding a third element effect on the cellular precipitation are explained in terms of horophilicity and horophobicity concepts.

The temperature effect on the cellular precipitation stages in the supersaturated solid solutions is clarified. When a solid solution is subjected to high temperatures, a primary cellular reaction creates favourable conditions to induce the secondary cellular reaction.

REFERENCES

1. L.N. Larikov and O.A. Shmatko, *Yacheistyy Raspad Peresyshchennykh Tverdykh Rastvorov* [Cellular Precipitation of Supersaturated Solid Solutions] (Kiev: Naukova Dumka: 1976) (in Russian).
2. N. Ageev, M. Hansen, and G. Sachs, *Z. Phys.*, **66**: 350 (1930); https://doi.org/10.1007/BF01390914
3. A.H. Geisler, *Phase Transformations in Solids* (New York: John Wiley & Sons: 1951).
4. H.K. Hardy and T.J. Heal, *Progress in Metal Physics*, 5: 143 (1954); https://doi.org/10.1016/0502-8205(54)90006-4
5. L.N. Larikov and O.A. Shmatko, *Metallofizika*, **33**: 5 (1971) (in Russian).
6. R. Watanabe, *Bull. Japan Inst. Metals*, **6**, No. 6: 435 (1967) (in Japanese).
7. D. Turnbull, *Acta. Metall.*, **3**, No. 1: 55 (1955); https://doi.org/10.1016/0001-6160(55)90012-2
8. K.N. Tu and D.B. Turnbull, *Acta Metall.*, **15**, No. 2: 369 (1967); https://doi.org/10.1016/0001-6160(67)90214-3
9. K.N. Tu and D.B. Turnbull, *Acta. Metall.*, **15**, No. 8: 1317 (1967); https://doi.org/10.1016/0001-6160(67)90007-7
10. K.N. Tu and D.B. Turnbull, *Acta. Metall.*, **17**, No. 10: 1263 (1969); https://doi.org/10.1016/0001-6160(69)90142-4
11. N.F. Voronina, P. Zięmba, A. Pawlowski, and O.A. Shmatko, *Met. Phys. Adv. Tech.*, **18**: 391 (1999).
12. A. Kelly and R.B. Nicholson, *Progress in Materials Science* (Oxford: Pergamon Press: 1963), vol. **10**, No. 3 p. 149.
13. S. Ibarra, Jr., *The Morphology of Cellular Precipitation in Aluminum Rich Aluminum−Silver Alloys* (Doctoral Dissertation: 1972); https://scholarsmine.mst.edu/doctoral_dissertations/193
14. R. Schaller and W. Benoit, *J. Phys. Colloques*, **42**, No. C5: 881 (1981); https://doi.org/10.1051/jphyscol:19815135
15. W. Gruhl and H. Kramer, *Metall*, **12**, No. 8: 707 (1958).
16. C.S. Smith, *Trans. ASM.*, **45**: 533 (1953).
17. V.M. Baranovskiy, M.E. Gurevich, L.N. Larikov, B.S. Khomenko, and O.A. Shmatko, *Metallofizika*, **27**: 65 (1970) (in Russian).

18. S.V. Divinski, S.M. Zakharov, and O.A. Shmatko, *Usp. Fiz. Met.*, **7**, No. 1: 1 (2006) (in Russian);
https://doi.org/10.15407/ufm.07.01.001
19. L.N. Larikov, Yu.N. Petrov and S.T. Borimskaya, *Voprosy Fiziki Metallov i Metallovedeniya*, **19**: 148 (1964) (in Russian).
20. L.N. Larikov and Yu.F. Yurchenko, *Ukr. Fiz. Zhurnal*, **9**, No. 12: 1345 (1964) (in Ukrainian).
21. L.N. Larikov and Yu.F. Yurchenko, *Teplovyye Svoistva Metallov i Splavov: Spravochnik* [Heat Properties of Metals and Alloys: Handbook] (Kiev: Naukova Dumka: 1985) (in Russian).
22. R.A. Fournelle and J.B. Clark, *Metal Trans.*, **3**, No. 11: 2757 (1972);
https://doi.org/10.1007/BF02652842
23. M.V. Itkin, V.S. Krasil'nikov, and O.A. Shmatko, *Metallofizika*, **7**, No. 6: 27 (1985) (in Russian).
24. N.I. Afanas'ev and T.F. Elsukova, *Fiz. Met. Metalloved.*, **53**, No. 2: 341 (1982) (in Russian).
25. D. Turnbull and H.N. Treaftis, *Acta Metall.*, **3**, No. 1: 43 (1955);
https://doi.org/10.1016/0001-6160(55)90011-0
26. G.R. Speich, *Trans. AIME*, **227**, No. 3: 754 (1963).
27. R.A. Fournelle, *Acta Metall.*, **27**, No. 7: 1135 (1979);
https://doi.org/10.1016/0001-6160(79)90131-7
28. R.A. Fournelle, *Acta Metall.*, **27**, No. 7: 1147 (1979);
https://doi.org/10.1016/0001-6160(79)90132-9
29. H. Tsubakino, *Mater. Sci. Lett.*, **1**, No. 7: 306 (1982);
https://doi.org/10.1007/BF00728862
30. K. Detert und H. Pohl, *Z. Metallkunde*, **57**, No. 2: 130 (1966).
31. P.J. Clemm and J.C. Fisher, *Acta Metall.*, **3**, No. 1: 70 (1955);
https://doi.org/10.1016/0001-6160(55)90014-6
32. M. Avrami, *Chem. Phys.*, **7**: 1103 (1939);
https://doi.org/10.1063/1.1750380
33. T.S. Gatsenko, *Metallofiz. Noveishie Tekhnol.*, **36**, No. 5: 705 (2014) (in Ukrainian);
https://doi.org/10.15407/mfint.36.05.0705
34. M.V. Itkin and O.A. Shmatko, *Doklady AN Ukr.RSR, Ser. A., Phys.-Math. Tech. Sci.*, No. 7: 66 (1980) (in Ukrainian).
35. Ya.B. Zel'dovich, *Zh. Eksp. Teor. Fiz.*, **12**, Nos. 11–12: 525 (1942) (in Russian).
36. W.A. Anderson and R.F. Mehl, *Trans. AIME*, **161**: 140 (1945).
37. M. Hillert, *The Mechanism of Phase Transformations in Crystalline Solids* (London: Institute of Metals: 1969), Monograph No. 33, p. 231.
38. M. Hillert, *Met. Trans.*, **3**, No. 11: 2729 (1972);
https://doi.org/10.1007/BF02652840
39. C. Zener, *Trans. AIME*, **167**, No. 5: 550 (1946).
40. J.W. Cahn, *Acta. Metall.*, **7**, No. 1: 18 (1959);
https://doi.org/10.1016/0001-6160(59)90164-6
41. R.G. Rose, *Acta Metall.*, **5**, No. 7: 404 (1957);
https://doi.org/10.1016/0001-6160(57)90010-X
42. M. Hillert and G.R. Purdy, *Acta Met.*, **26**, No. 2: 333 (1978);
https://doi.org/10.1016/0001-6160(78)90132-3
43. T.S. Gatsenko, E.O. Maksimenko, M.I. Savchuk and O.A. Shmatko, *Metallofiz. Noveishie Tekhnol.*, **34**, No. 5: 51 (2012) (in Ukrainian).
44. H.I. Aaronson and Y.C. Liu, *Scr. Met.*, **2**, No. 1: 1 (1968);
https://doi.org/10.1016/0036-9748(68)90157-9

45. J. Petermann und E. Hornbogen, *Z. Metallkunde*, **59**, No. 11: 814 (1968).

46. B. Sunquist, *Acta Met.*, **16**, No. 12: 1413 (1968);
https://doi.org/10.1016/0001-6160(68)90037-0

47. F.M. Carpay, *Acta Met.*, **19**, No. 12: 1279 (1971);
https://doi.org/10.1016/0001-6160(71)90061-7

48. M.I. Savchuk, T.S. Gatsenko, M.I. Dzyublenko, and O.A. Shmatko, *Metallofiz. Noveishie Tekhnol.*, **34**, No. 2: 189 (2012) (in Ukrainian).

49. J.W. Cahn, *Acta Met.*, **4**, No. 5: 449 (1956);
https://doi.org/10.1016/0001-6160(56)90041-4

50. D. Turnbull and H.N. Treaftis, *Trans. Met. Soc. AIME*, **212**, No. 1: 33 (1958).

51. L.N. Larikov, B.I. Nikolin, N.N. Shevchenko, and O.A. Shmatko, *Metallofizika*, **3**, No. 2: 40 (1981) (in Russian).

52. S.M. Kedrovsky, Yu.M. Koval, V.M. Slipchenko, K.V. Slipchenko, and O.V. Fila-tov, *Metallofiz. Noveishie Tekhnol.*, **37**, No. 2: 199 (2015) (in Russian);
https://doi.org/10.15407/mfint.37.02.0199

53. L.N. Larikov and O.A. Shmatko, *Metallofizika*, **37**: 63 (1971) (in Russian).

54. A. Filatov, A. Pogorelov, D. Kropachev, and O. Dmitrichenko, *Defect Diffus. Forum*, **363**: 173 (2015);
https://doi.org/10.4028/www.scientific.net/DDF.363.173

55. A.V. Filatov, D.A. Kropachev, and A.E. Pogorelov, *Metallofiz. Noveishie Tekh-nol.*, **35**, No. 6: 793 (2013) (in Russian).

56. O.V. Filatov and O.M. Soldatenko, *Metallofiz. Noveishie Tekhnol.*, **42**, No. 1: 1 (2020);
https://doi.org/10.15407/mfint.42.01.0001

57. V.E. Danilchenko, A.V. Filatov, V.F. Mazanko, and V.E. Iakovlev, *Nanoscale Res. Lett.*, **12**: 194. (2017);
https://doi.org/10.1186/s11671-017-1978-z

58. V.Y. Bondar, V.E. Danilchenko, V.F. Mazanko, O.V. Filatov, and V.E. Iakovlev, *Usp. Fiz. Met.*, **19**, No. 1: 70 (2018);
https://doi.org/10.15407/ufm.19.01.070

59. V.Yu. Danilchenko, V.F. Mazanko, O.V. Filatov, and V.E. Iakovlev, *Usp. Fiz. Met.*, **20**, No. 3: 426 (2019);
https://doi.org/10.15407/ufm.20.03.426

60. Yu.M. Koval', A.M. Bezugliy, M.I. Didik, N.V. Zaytseva, and O.A. Shmatko, *Dopovidi NAN Ukr.*, **2**: 102 (2004) (in Ukrainian).

61. S.P. Vorona, V.F. Mazanko, M.I. Savchuk, K.M. Khranovska, I.O. Shmatko, and O.A. Shmatko, *Metallofiz. Noveishie Tekhnol.*, **37**, No. 1: 103 (2015) (in Ukrainian);
https://doi.org/10.15407/mfint.37.01.0103

62. M.I. Savchuk, I.O. Shmatko, and O.A. Shmatko, *Abstr. Int. Conf. MRF (October 14−17, 2014, Kharkiv)* (Kharkiv: 2014), p. 38.

63. M.I. Savchuk, *Stadiynist' ta Kinetiko-Termodynamichni Zakonomirnosti Komir-kovykh Reaktsiy v Splavakh Svynets'−Olovo* (Author's Abstract of Disser. for Cand. Sci. (Phys.-Math.)) (Kyiv: G.V. Kurdyumov Institute for Metal Physics, N.A.S.U.: 2016) (in Ukrainian).

64. A.K. Kuznyak, M.I. Savchuk, I.O. Shmatko, and O.A. Shmatko, *Abstr. Int. Conf. 'Evrika' (May. 16−18, 2017, Lviv)* (Lviv: 2017), p. D7.

65. M.I. Savchuk and O.A. Shmatko, *Abstr. Int. Conf. 'Evrika' (May 15−17, 2018, Lviv)* (Lviv: 2018), p. D9.

66. M.I. Savchuk and O.A. Shmatko, *Abstr. Int. Conf. (October 11, 2019, Kyiv)* (Kyiv: 2019), p. 10.

67. M.I. Savchuk and O.A.Shmatko, *Abstr. Int. Conf. (September 8−9, 2018, Kiev)* (Kiev: 2018), p. 48.

68. T.V. Efimova, A.L. Larikov, V.G. Tinyaev, I.O. Shmatko, and O.A. Shmatko, *Metallofizika*, **6**, No. 5: 67 (1984) (in Russian).
69. N.I. Afanas'ev and T.F. Elsukova, *Fiz. Met. Metalloved.*, **57**, No. 1: 96 (1984) (in Russian).
70. T.S. Gatsenko, Yu.O. Lyashenko, and O.A. Shmatko, *Visnyk Cherkas'kogo Natsional'nogo Universytetu*, **269**: 31 (2013) (in Ukrainian).
71. S.N. Zadumkin, *Zhurnal Neorganicheskoy Khimii*, **5**: No. 8: 1892 (1960) (in Russian).
72. V.I. Arkharov, *Teoriya Mikrolegirovaniya Splavov* [Theory of Microalloying] (Moscow: Mashinostroenie: 1975) (in Russian).

М.І. Савчук, О.В. Філатов, О.А. Шматко
Інститут металофізики ім. Г.В. Курдюмова НАН України,
бульв. Академіка Вернадського, 36, 03142 Київ, Україна

ФІЗИЧНІ ЗАКОНОМІРНОСТІ КОМІРКОВОГО РОЗПАДУ
ПЕРЕСИЧЕНИХ ТВЕРДИХ РОЗЧИНІВ НА ОСНОВІ Co, Cu ТА Pb

Розглядається питання розпаду пересичених твердих розчинів за комірковим механізмом з точки зору фізичних закономірностей даного явища. Описано загальні характеристики процесу. Частково описано механізми зародкоутворення та подальшого росту комірок, а також кінетичні параметри процесів. Охарактеризовано впливи деяких зовнішніх чинників на перебіг коміркового розпаду та стадійність даного процесу. Зокрема, вивчено вплив температури гартівного середовища, а також вплив третього елемента на процес коміркового розпаду.

Ключові слова: пересичені тверді розчини, старіння, комірковий розпад, лямельна структура, кінетичні параметри, стадійність розпаду.